

Constraining The Density Dependence Of The Symmetry Energy Using The Multiplicity And Average P_T Ratios Of Charged Pions

Dan Cozma*

IFIN-HH, Reactorului 30, 077125 Măgurele-Bucharest, Romania

E-mail: dan.cozma@theory.nipne.ro

The charged pion multiplicity ratio in intermediate energy heavy-ion collisions, a probe of the density dependence of symmetry energy above the saturation point, has been proven in a previous study to be extremely sensitive to the strength of the isovector $\Delta(1232)$ potential in nuclear matter. As there is no current knowledge, either from theory or experiment, about the magnitude of this quantity, the extraction of constraints for the slope of the symmetry energy at saturation by using exclusively the mentioned observable is hindered at present. It is shown that, by including the ratio of average p_T of charged pions $\langle p_T^{(\pi^+)} \rangle / \langle p_T^{(\pi^-)} \rangle$ in the list of fitted observables, the noted problem can be circumvented. A realistic description of this observable requires the accounting for the interaction of pions with the dense nuclear matter environment embodied by the so called S and P-wave pion optical potentials. This is performed within the framework of a QMD transport model that enforces the conservation of the total energy of the system and incorporates information about these potentials gained by the experimental study of pionic atoms and pion-nucleus scattering and also from theoretical hadronic models and chiral perturbation theory. A symmetry energy with a value of the slope parameter $L > 50$ MeV is favored, at 1σ confidence level, from a comparison with published FOPI experimental data. Future experimental measurements of pionic observables will present the opportunity of extracting a more precise constraint for the symmetry energy stiffness by restricting the comparison to low momentum pions and reducing the model dependence induced by uncertainties in the density dependence of the pion optical potential by studying also heavy-ion collisions of isospin symmetric nuclei.

PoS (INPC2016) 346

*The 26th International Nuclear Physics Conference
11-16 September, 2016
Adelaide, Australia*

*Speaker.

1. Introduction

Pions produced in intermediate energy heavy-ion collisions have been shown to provide promising means for the study of the isovector part of the equation of state of nuclear matter (asy-EoS), commonly known as the symmetry energy (SE). In particular, the ratio of multiplicities of charged pions (PMR) has been demonstrated to be sensitive to the density dependence of the SE in the supranormal density region while uncertainties in the isoscalar part of the equation of state are suppressed [1].

Attempts to constrain the density dependence of the SE, in particular its slope L at saturation, using this observable have made use of existing experimental data for pion production in central ($b < 2.0$ fm) $^{197}\text{Au} + ^{197}\text{Au}$ collisions at an impact energy of 400 MeV/nucleon due to FOPI Collaboration [2, 3]. Studies performed making use of different available transport models have resulted in an inconsistent picture: constraints on the high density dependence of the SE ranging from a very soft to a stiff one have been extracted [4, 5, 6], or even no sensitivity on the slope parameter has been reported [7]. Additionally, most models have led to a contradiction between the π^-/π^+ multiplicity ratio and neutron/proton elliptic flow ratio extracted constraints for the SE stiffness.

Efforts to understand this discrepancy by studying the impact of in-medium modifications of the pion-nucleon interaction, the kinetic part of the SE term, the neutron skin thickness, or particle production threshold shifts due to the inclusion of self-energy contributions on the PMR value have proven, from a quantitative point of view, largely unsuccessful. Studies of the impact of self-energy contributions in the energy conservation constraint that appears in the collision term of transport equations have however proven more fruitful [8, 9]. They lead to shifts of particle production thresholds inside a dense nuclear medium and impose the conservation of the total energy of the participants of a binary collision. Regarding the impact on PMR, a stiff asy-EoS leads to a higher value for this observable than a soft choice does. This is in opposition with the situation when these effects are not taken into account.

Requiring that the total energy of the entire system be conserved leads to an enhancement of the impact of self-energies (or equivalently potential energies in nuclear matter) on particle production thresholds [10] leading to important modifications of pion multiplicity predictions, particularly for the π^- meson, while maintaining the sensitivity of the PMR to SE density dependence. As a result, constraints for its stiffness in agreement with those extracted from elliptic flow observables can be obtained within the scenario of total energy conservation of the system for the standard choice for the $\Delta(1232)$ potentials in nuclear matter. A strong dependence of the results on the strength of the isovector $\Delta(1232)$ potential in nuclear matter has however been reported. Owing to the fact that the magnitude of this quantity is presently unknown, the extraction of information on the asy-EoS solely from PMR is consequently hindered at present.

The contribution was devoted to presenting the results of a recent study [11] which extends the analysis performed in Ref. [10] to the average p_T ratio of charged pions $\langle p_T^{(\pi^+)} \rangle / \langle p_T^{(\pi^-)} \rangle$ (PAPTR). It is shown that by using the two observables, PMR and PAPTR, constraints for both the symmetry energy stiffness and strength of the isovector $\Delta(1232)$ potential can simultaneously be extracted from available experimental data. To achieve that goal, the model of Ref. [10] has further been improved by accounting for the interaction between pions and dense nuclear matter, described by the so called S and P-wave pion optical potential. The present proceeding contribution provides

a short account of the implemented modifications to the transport model and the most relevant results obtained in connection to constraining the density dependence of SE. All the findings of the reported study are presented in great details in Ref. [11].

2. The model

Heavy-ion collision dynamics is simulated using an upgraded version [10] of the Tübingen quantum molecular dynamics Model (QMD) transport model. It allows the enforcing of conservation of the total energy of the system during an event, by including potential energies in the energy conservation constraint imposed when determining the final state of a 2-body scattering, decay or absorption process,

$$\sum_j \sqrt{p_j^2 + m_j^2} + U_j = \sum_i \sqrt{p_i^2 + m_i^2} + U_i, \quad (2.1)$$

both indexes running over all particles present in the system and corresponding, from left to right, to the final and initial states of an elementary reaction. This scenario has been referred to as the “global energy conservation” (GEC) scenario in [10]. Additionally, the “local energy conservation” (LEC) and “vacuum energy conservation” (VEC) scenarios have been introduced. They correspond to the situation when only the potential energies of the particles directly involved in the 2-body scattering, decay or absorption process are accounted for in the energy conservation constraint and when the potential energies of particles in the medium are ignored in the collision term [10], respectively.

The Gogny-inspired parametrization of the equation of state of nuclear matter [12] has been selected to describe the mean-field experienced by a nucleon at finite density. It leads to a mean-field nucleon potential,

$$U(\rho, \beta, p, \tau, x) = A_u(x) \frac{\rho_{\tau'}}{\rho_0} + A_l(x) \frac{\rho_{\tau}}{\rho_0} + B \left(\frac{\rho}{\rho_0} \right)^{\sigma} (1 - x\beta^2) - 8\tau x \frac{B}{\sigma+1} \frac{\rho^{\sigma-1}}{\rho_0^{\sigma}} \beta \rho_{\tau'} \quad (2.2)$$

$$+ \frac{2C_{\tau\tau}}{\rho_0} \int d^3 \vec{p}' \frac{f_{\tau}(\vec{r}, \vec{p}')}{1 + (\vec{p} - \vec{p}')^2 / \Lambda^2} + \frac{2C_{\tau\tau'}}{\rho_0} \int d^3 \vec{p}' \frac{f_{\tau'}(\vec{r}, \vec{p}')}{1 + (\vec{p} - \vec{p}')^2 / \Lambda^2},$$

that displays besides density (ρ) and isospin asymmetry (β) also a momentum (p) dependence in both the isoscalar and isovector components (τ). The parameter x has been introduced to allow for adjustments of the symmetry energy stiffness. Negative and positive values of this parameter correspond to a stiff and a soft density dependence, respectively. The values of the $C_{\tau\tau}$, $C_{\tau\tau'}$ and Λ parameters are determined by optimally reproducing the momentum dependent part of the Gogny interaction [12]. This results in an effective isoscalar nucleon mass of $0.7m_N$ and a neutron-proton effective mass splitting of approximately 0.4β at saturation density. The remaining parameters are determined from the location of the saturation point (ρ_0), binding energy at saturation, magnitude of the symmetry energy at saturation ($S_0=30.6$ MeV) and value of the compressibility modulus ($K=245$ MeV).

The expression of the potential of $\Delta(1232)$ and heavier baryonic resonances in nuclear matter is derived under the assumption that it is given by the weighted average of that of neutrons and protons, the weight for each charge state being equal to the square of the Clebsch-Gordon coefficient

for isospin coupling in the process $\Delta \rightarrow \pi N$. It can be cast in the following form,

$$\begin{aligned} V_{\Delta^-} &= V_N + (3/2)V_v \\ V_{\Delta^0} &= V_N + (1/2)V_v \\ V_{\Delta^+} &= V_N - (1/2)V_v \\ V_{\Delta^{++}} &= V_N - (3/2)V_v, \end{aligned} \quad (2.3)$$

where V_N and V_v are the isoscalar nucleon potential and the difference between the potentials of two neighboring isospin partners respectively. It can be shown that $V_v = \delta$, with the definition $\delta = (1/3)(V_n - V_p)$. By varying the magnitude of V_v different scenarios for the strength of the isovector baryon potential can be explored. The choices $V_v = -2\delta, -\delta, 0, \delta, 2\delta$ and 3δ have been used in this study.

The interaction of pions with the dense nuclear environment is accounted for by including the effect of the so called S and P-wave pion optical potentials in the transport equations. A widely used parametrization for these quantities, introduced by Ericson and Ericson, reads

$$V_{opt}(r) = \frac{2\pi}{\mu} \left[-q(r) + \vec{\nabla} \frac{\alpha(r)}{1 + \frac{4}{3}\pi\lambda\alpha(r)} \vec{\nabla} \right] \quad (2.4)$$

where

$$\begin{aligned} q(r) &= \varepsilon_1(\bar{b}_0\rho + \bar{b}_1\beta\rho) + \varepsilon_2B_0\rho^2, \\ \alpha(r) &= \varepsilon_1^{-1}(c_0\rho + c_1\beta\rho) + \varepsilon_2^{-1}(C_0\rho^2 + C_1\beta\rho^2). \end{aligned}$$

Here μ is the reduced mass of the pion-nucleus system while λ is the Lorentz-Lorentz correction parameter which accounts for the impact of short-range nucleon-nucleon correlations on the potential. The extra parameters are defined as follows: $\varepsilon_1 = 1 + m_\pi/m_N$, $\varepsilon_2 = 1 + m_\pi/2m_N$, with m_π and m_N the π -meson and nucleon masses respectively. The parameters \bar{b}_0 , \bar{b}_1 and B_0 determine the strength of the S-wave part of the interaction, while the P-wave term is described by the ones labeled c_0 , c_1 , C_0 and C_1 . Their values are determined from a comparison to experimental data for bound states of pionic atoms and elastic pion-nucleon scattering [13]. An extraction of their values from a comparison with theoretical effective hadronic models usually reveals a missing strength in the P-wave component of the latter. Parameter set values used in the current study can be read from Table. II in Ref. [11]. They are a subset of those listed in Ref. [13] and were selected in order to cover with a minimum number of parameter sets the uncertainties in the density dependence of these potentials.

These potentials need to be extrapolated at energies far above those probed in pionic atoms in order to be applicable to heavy-ion related studies. This is particularly true for the P-wave component which shows a strong energy dependence already at small energies, as induced by the energy dependence of the $\Delta(1232)$ decay width. To that end we mirror the energy dependence of a theoretical P-wave potential model [14], based on a local approximation of the delta-hole model, that allows a good description of elastic pion-nucleus data up to pion kinetic energies of about 300 MeV. In practice, this is achieved by multiplying the P-wave part of the potential of Eq. (2.4) by the form factor,

$$f(p^2) = \frac{1.0 - p_{eff}^2/\Lambda_1^2 + p_{eff}^4/\Lambda_2^4}{1.0 - p^2/\Lambda_1^2 + p^4/\Lambda_2^4}, \quad (2.5)$$

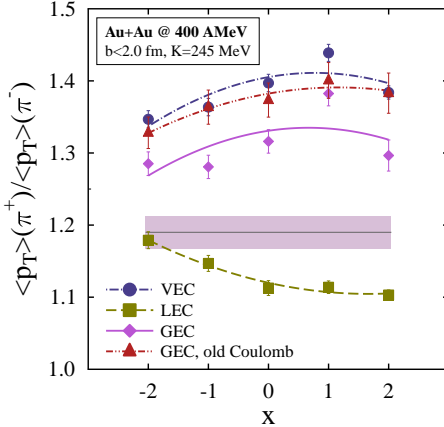


Figure 1: Average p_T ratio of charged pions as a function of the stiffness parameter x in central $^{197}\text{Au} + ^{197}\text{Au}$ collision at an impact energy of 400 MeV/nucleon. Results for the VEC (dashed-dotted curves), LEC (dashed curves) and GEC scenarios are presented. For the case of the GEC scenario results for two strengths of the Coulomb interaction are shown: the one of Ref. [10] (dashed-double-dotted curves) and the one used in this study (full curves). The FOPI experimental result for the PAPTR [2] is depicted by a horizontal band.

with $\Lambda_1 = 0.55$ GeV and $\Lambda_2 = 0.22$ GeV. For the S-wave component of the pion optical potential the energy dependence is less pronounced and for the parametrizations extracted from pionic atom data it is completely ignored. Alternatively, a parametrization of the S-wave potential, constructed by using results from chiral perturbation theory [16, 17], effective hadronic models [15] and experimental pion-nucleus scattering [18], can be used as it features also a moderate energy dependence

$$\begin{aligned} b_0(\omega) &= -0.010 - 0.00016\omega, & \bar{b}_0 &= b_0 - \frac{3}{2\pi}(b_0^2 + 2b_1^2)\left(\frac{3\pi^2}{2}\rho\right)^{1/3} \\ b_1(\rho) &= -0.088\left(1 + \frac{0.6116}{b_1}\frac{\rho}{\rho_0}\right), & \bar{b}_1 &= b_1. \end{aligned} \quad (2.6)$$

Here ω denotes the pion kinetic energy and the potential parameters b_0 and b_1 are expressed in units of $[m_\pi^{-1}]$.

3. Selected results

The impact that the various energy conservation scenarios, briefly described in Section 2, have on average p_T ratios of pions is presented in Fig. (1). VEC and GEC scenario simulations reveal values of PAPTR that overshoot the experimental FOPI result [2] by 10-20%. On the other hand the LEC scenario leads to PAPTR values below their experimental counterpart by at most 10%. The impact of local energy conservation (as compared to VEC) is therefore much more pronounced for PAPTR than for multiplicity ratios, while the difference between LEC and GEC scenarios is equally dramatic for these two observables. A moderate dependence of PAPTR on the SE stiffness is also demonstrated, a softer asy-EoS leading to a higher PAPTR for the VEC and GEC scenarios and the opposite for LEC.

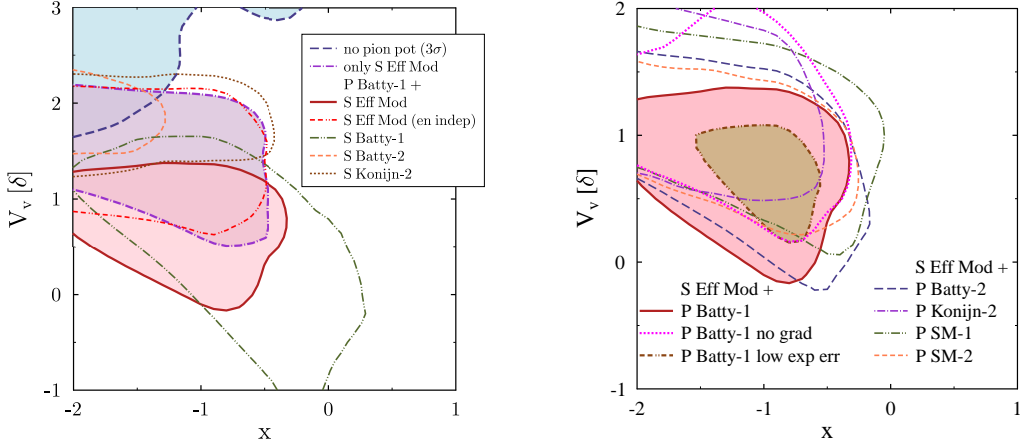


Figure 2: Sensitivity of the extracted constraints for the stiffness parameter x and strength of the isovector $\Delta(1232)$ potential V_v to different choices for the S -wave (left panel) and P -wave (right panel) pion potentials. The calculations help quantify the impact of uncertainties in the energy and density dependence of these potentials on the quantities of interest. The case for which pion potential contributions are completely omitted (“no pion pot”) or only the S -wave component is included (“only S Eff Mod”) are also shown (left panel). Result for a version of the P -wave potential with the gradient terms omitted is also shown (“ P Batty-1 no grad” in the right panel).

The impact of each of the pion optical potential components on pion multiplicities, pion average transverse momenta and their corresponding ratios is studied in great detail in Ref. [11]. It is found that while their impact on PMR is only moderate in relative terms, their omission would lead to uncertainties in the extracted values of the slope L of the symmetry energy of as much as 50 MeV for certain fixed values of the isovector $\Delta(1232)$ potential strength. The impact of the S and P -wave pion potentials on PAPTR amounts to about 20% and 10% respectively and their inclusion is crucial for reaching an agreement with the experimental value. A similar statement holds true when comparing to experimental data for the absolute average transverse momenta.

The results presented in Fig. (1) demonstrate the sensitivity of PAPTR to the asy-EoS stiffness, even though it is not a pronounced as for PMR. Owing to a different dependence on the strength of the isovector $\Delta(1232)$ potential [11], the two observables can be used simultaneously to extract constraints for both quantities of interest. This is demonstrated in Fig. (2) where the 1σ confidence level (CL) contour plots of the quantity χ^2/dof determined by comparing theoretical and experimental results for the observables PMR and PAPTR for different choices for the pion S -wave (left panel) and P -wave (right panel) potentials are plotted.

The experimental values for PMR and PAPTR cannot be reproduced simultaneously if contributions due to the pion optical potential are omitted (left panel of Fig. (2)). In fact, most of the probed parameter space lies outside the 3σ CL region (curve labeled “no pion pot”). By including the S -wave potential the situation improves considerably (curve labeled “only S Eff Mod”). The inclusion of the P -wave potential has a clearly noticeable effect only on the favored value for the strength of the $\Delta(1232)$ isovector potential. The extracted constraints show however a pronounced sensitivity to the parametrization, and hence density dependence, used for the S -wave potential. Its energy dependence impacts mostly the extracted constraint for the strength of the isovector $\Delta(1232)$

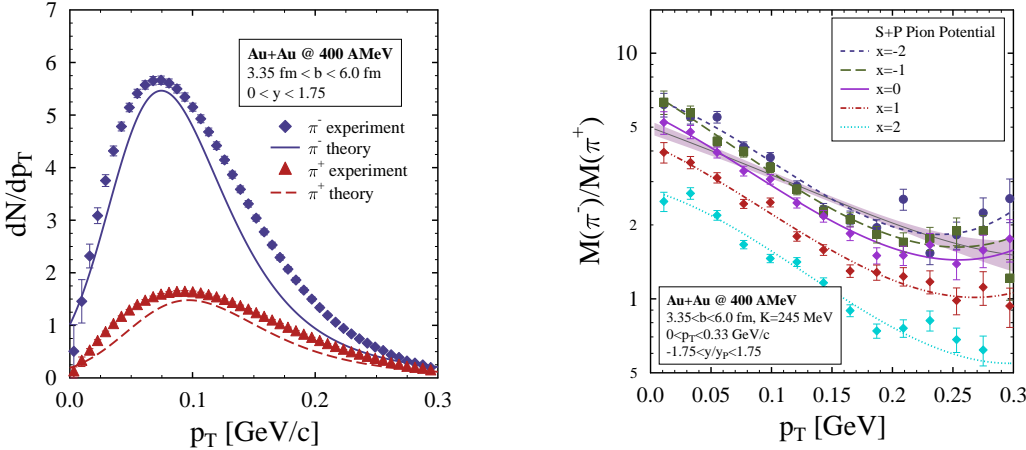


Figure 3: Comparison of theoretical transverse momentum spectra of charged pions (left panel) and transverse momentum dependent PMR (right panel) in mid-central $^{197}\text{Au} + ^{197}\text{Au}$ collisions at an impact energy of 400 MeV/nucleon to the FOPI Collaboration experimental data [19]. The effective model S -wave and the Batty-1 P -wave pion potentials have been accounted for in the simulations.

POS (INPC2016) 346

potential (compare full and double-dashed-double-dotted curves in the left panel of Fig. (2)).

The sensitivity of the extracted constraints for the SE stiffness to the parametrization used for the P -wave potential is presented in the right panel of Fig. (2). The uncertainty on the extracted value of the slope parameter L is of the order of 20 MeV (compare the contour plots for the “Batty-2”, “Konijn-2”, “SM-1” and “SM-2” P -wave parametrizations [13]), much less than the one induced by uncertainties in the density dependence of the S -wave potential. A similar conclusion holds true for the extracted constraint for the strength of the isovector $\Delta(1232)$ potential. Density gradient terms of the P -wave potential are shown to have noticeable impact only on this latter quantity. Additionally, it is shown that higher precision experimental data have the potential to lead to a considerably more precise constraint for the stiffness of the asy-EoS. This is achieved by artificially reducing the uncertainties of the existing experimental data for PMR and PAPTR to from 9% to 3% and from 2.5 % to 1.5% respectively (compare full and double-dashed-double-dotted curves).

In Fig. (3) a comparison of the transverse momentum spectra and transverse momentum dependent PMR with their experimental counterpart is presented. For these cases the strength of the isovector Δ potential has been set to $V_v=0.5 \delta$ in agreement with the favored constraints presented above. The description of the experimental data for the former observable is qualitatively good, the discrepancy between theory and experiment showing however a rather pronounced p_T dependence. This is enhanced for the case of the p_T dependent PMR, the extracted constraint for the stiffness parameter x depending strongly on the chosen window in transverse momentum. The result underlines the importance of energy dependence of the pion potential used in simulations and which is currently accurately known only for small values of the pion momentum. To circumvent this problem a comparison of theoretical predictions and future experimental data will have to be restricted only to pions of low momenta. For this case only, extrapolations of the pion potential extracted from pionic atom experiments will be fully justified.

4. Concluding remarks

The presented study has demonstrated that the extraction of constraints for the symmetry energy stiffness from pionic observables measured in intermediate energy heavy-ion collisions is viable. In order to circumvent the earlier noted problem of unknown strength of the isovector $\Delta(1232)$ potential in nuclear matter, the list of observables has been extended to include both the pion multiplicity ratio and the average p_T ratio. To convincingly describe the latter, contributions of the S and P-wave pion optical potentials have to be accounted for in the transport model of choice. In agreement with results of a previous study, the conservation of the total energy of the system is of crucial importance as well. With these ingredients in place a consistent description of the available experimental data is possible and meaningful constraints for the slope of the symmetry energy can be extracted, with $L > 50$ MeV at 1σ confidence level. A rather strong model dependence, originating from uncertainties in the density and energy dependence of the pion potentials, of the extracted constraints is however evidenced. The latter can be alleviated by restricting the study to low momentum pions, while for the former the study of heavy-ion collisions of isospin symmetric nuclei may prove helpful.

References

- [1] B. A. Li, G. C. Yong and W. Zuo, *Phys. Rev. C* **71** (2005) 014608.
- [2] W. Reisdorf et al. (FOPI), *Nucl. Phys. A* **781** (2007) 459.
- [3] W. Reisdorf et al. (FOPI), *Nucl. Phys. A* **848** (2010) 366.
- [4] Z. Xiao, B. A. Li, L. W. Chen, G. C. Yong and M. Zhang, *Phys. Rev. Lett.* **102** (2009) 062502.
- [5] W. J. Xie, J. Su, L. Zhu and F. S. Zhang, *Phys. Lett. B* **718** (2013) 1510.
- [6] Z. Q. Feng and G. M. Jin, *Phys. Lett. B* **683** (2010) 140.
- [7] J. Hong and P. Danielewicz, *Phys. Rev. C* **90** (2014) 024605.
- [8] G. Ferini, T. Gaitanos, M. Colonna, M. Di Toro and H. H. Wolter, *Phys. Rev. Lett.* **97** (2006) 202301.
- [9] T. Song and C. M. Ko, *Phys. Rev. C* **91** (2015) 014901.
- [10] M. D. Cozma, *Phys. Lett. B* **753** (2016) 166.
- [11] M. D. Cozma, *Phys. Rev. C* **95** (2017) 014601.
- [12] C. B. Das, S. D. Gupta, C. Gale and B. A. Li, *Phys. Rev. C* **67** (2003) 034611
- [13] K. Itahashi *et al.*, *Phys. Rev. C* **62** (2000) 025202.
- [14] C. Garcia-Recio, E. Oset, L. L. Salcedo, D. Strottman and M. J. Lopez, *Nucl. Phys. A* **526** (1991) 685.
- [15] M. Krell and T. E. O. Ericson, *Nucl. Phys. B* **11** (1969) 521.
- [16] W. Weise, *Acta Phys. Polon. B* **31** (2000) 2715.
- [17] W. Weise, *Nucl. Phys. A* **690** (2001) 98.
- [18] C. Garcia-Recio and E. Oset, *Phys. Rev. C* **40** (1989) 1308.
- [19] W. Reisdorf (FOPI Collaboration), *private communication* (2015).